

Rayleigh Regression Model for Ground Type Detection in SAR Imagery

B. G. Palm* F. M. Bayer† R. J. Cintra‡ M. I. Pettersson§ R. Machado¶

Abstract

This letter proposes a regression model for nonnegative signals. The proposed regression estimates the mean of Rayleigh distributed signals by a structure which includes a set of regressors and a link function. For the proposed model, we present: (i) parameter estimation; (ii) large data record results; and (iii) a detection technique. In this letter, we present closed-form expressions for the score vector and Fisher information matrix. The proposed model is submitted to extensive Monte Carlo simulations and to measured data. The Monte Carlo simulations are used to evaluate the performance of maximum likelihood estimators. Also, an application is performed comparing the detection results of the proposed model with Gaussian-, Gamma-, and Weibull-based regression models in SAR images.

Keywords

Detection, Rayleigh distribution, regression model, reparameterized Rayleigh distribution, SAR images.

1 Introduction

The classical linear regression model is commonly employed to estimate an unknown and deterministic parameter vector β in the linear equation $\mathbf{y} = \mathbf{H}\beta + \mathbf{e}$. The quantity \mathbf{y} is defined as the observed output signal, \mathbf{H} is a linear transformation, and \mathbf{e} is a Gaussian noise vector [26]. However, in situations where the observed output signal is asymmetric, continuous, and nonnegative, as in Rayleigh distributed signals, inference methods based on the Gaussian assumption can lead to misleading results. Indeed, the Rayleigh distribution is widely used in signal and image processing, as in [4, 11, 16, 20, 21, 27].

One important application for the Rayleigh distribution is in the context of synthetic aperture radar (SAR) image modeling, where this distribution can be employed for characterizing amplitude values of image pixels [7, 10, 16]. A common problem in SAR image processing is the identification and classification of distinct targets or land uses in images [2, 6]. Usually, these problems are treated assuming homogeneity of the regions. However, the use of regression models adopting suitable distributions without assuming homogeneity in the images can generate accurate results for the above SAR-related challenges, as presented by [24].

In this paper, our goal is two-fold. First, we propose a regression model for non-Gaussian situations, where the observed output signal is asymmetric and measured continuously on the real positives values. For the proposed model, we introduce parameter estimation, large data record results, and goodness-of-fit measures. Second, we introduce a change detector for the amplitude values of non-Gaussian SAR images. Detection problems are commonly treated assuming Gaussian distribution to the signals. However, SAR images are usually non-Gaussian, prompting the use of the Rayleigh distribution to yield more accurate results for detection problems. Thus, the present letter introduce a detector based on the asymptotic properties of the proposed Rayleigh regression model estimators.

The letter is organized as follows. In Section 2, we introduce the proposed model and present the score vector, and the goodness-of-fit measures. Section 3 shows the Fisher information matrix and the proposed detector. Section 4 presents Monte Carlo simulations and an application for SAR images. Finally, the conclusion of this work can be found in Section 5.

*Programa de Pós-graduação em Estatística, Universidade Federal Pernambuco, Brazil and the Department of Mathematics and Natural Sciences, Blekinge Institute of Technology, Sweden (E-mail: brunagpalm@gmail.com).

†Departamento de Estatística and LACESM, Universidade Federal de Santa Maria, Brazil (E-mail: bayer@ufsm.br).

‡Signal Processing Group, UFPE, Brazil. (E-mail: rjpsc@de.ufpe.br).

§Department of Mathematics and Natural Sciences, Blekinge Institute of Technology, Sweden (E-mail: mats.pettersson@bth.se).

¶Department of Telecommunications, Aeronautics Institute of Technology (ITA), São José dos Campos - SP, Brazil (E-mail: rmachado@ita.br).

2 Proposed Rayleigh Regression Model

Let y be a random variable with Rayleigh distribution. Its probability density function (pdf) is given by [9, p. 30], [7]:

$$p(y; \sigma) = \frac{y}{\sigma^2} \exp\left(-\frac{y^2}{2\sigma^2}\right), \quad y \geq 0,$$

where $\sigma > 0$ is the parameter. The mean and the variance of y are given by

$$\mathbb{E}(y) = \sigma \sqrt{\frac{\pi}{2}} \quad \text{and} \quad \text{Var}(y) = \sigma^2 \left(\frac{4-\pi}{2}\right).$$

Although the Rayleigh density is commonly governed by the parameter σ , regression models usually characterize the mean of the response signal [13], which has a more direct interpretation than σ . Thus, we consider a reparametrization of the Rayleigh distribution in terms of the mean of the response signal and its regression structure.

2.1 Reparametrization of the Rayleigh Distribution

Considering the parameterization $\mu = \sigma \sqrt{\frac{\pi}{2}}$, we have the following pdf of the mean-based Rayleigh distribution:

$$f(y; \mu) = \frac{\pi y}{2\mu^2} \exp\left(-\frac{\pi y^2}{4\mu^2}\right), \quad y \geq 0, \quad (1)$$

where $\mu > 0$ is the mean parameter. The cumulative distribution function is given by

$$F(y; \mu) = 1 - \exp\left(-\frac{\pi y^2}{4\mu^2}\right).$$

The quantile function, useful for generating pseudo-random occurrences in inversion method, is given by

$$Q(u; \mu) = 2\mu \sqrt{\frac{-\log(1-u)}{\pi}}.$$

The mean and variance of y are given by

$$\mathbb{E}(y) = \mu \quad \text{and} \quad \text{Var}(y) = \mu^2 \left(\frac{4}{\pi} - 1\right).$$

2.2 Regression Model

Let $y[1], y[2], \dots, y[N]$ be N independent random samples, where each sample follows the Rayleigh density in (1) with mean $\mu[n]$, $n = 1, 2, \dots, N$. The proposed Rayleigh regression model is obtained by considering a linear predictor $\eta[n]$ for the mean of $y[n]$ furnished by

$$\eta[n] = g(\mu[n]) = \sum_{i=1}^r \beta_i x_i[n], \quad n = 1, 2, \dots, N, \quad (2)$$

where $r < N$ is the number of covariates considered in the model, $\beta = (\beta_1, \beta_2, \dots, \beta_r)^\top$ is a vector of unknown linear parameters, $\mathbf{x}[n] = (x_1[n], x_2[n], \dots, x_r[n])^\top$ is a vector of deterministic independent variables, and $g(\cdot)$ is a strictly monotonic and twice differentiable link function where $g: \mathbb{R}^+ \rightarrow \mathbb{R}$. If the intercept is considered, then $x_1[n] = 1$. The link function $g(\cdot)$ relates the linear predictors $\eta[n]$ to the expected value $\mu[n]$ of data $y[n]$. When $\mu[n] > 0$, a common choice of link function is the log link $\log(\mu[n]) = \eta[n]$ with its inverse $\mu[n] = \exp(\eta[n])$.

The proposed model is similar to the generalized linear models (GLM) [13], except for the fact that the Rayleigh density cannot be written in the canonical form of the exponential family of distributions. A regression model considering the

Rayleigh distribution is also presented in [1]. However, the proposed model is based on the standard Rayleigh distribution parametrization. In addition, in this letter, the maximum likelihood (ML) method [17, Ch. 2] based on the reparametrized Rayleigh distribution is considered to obtain the regression parameters estimates, as presented in the next section.

2.3 Likelihood Inference

Parameter estimation of the Rayleigh regression model can be performed by the maximum likelihood method [17, Ch. 2]. The ML estimates are given by

$$\hat{\boldsymbol{\beta}} = \arg \max_{\boldsymbol{\beta}} \ell(\boldsymbol{\beta}),$$

where $\ell(\boldsymbol{\beta})$ is the log-likelihood function of the parameters for the observed signal, defined as $\ell(\boldsymbol{\beta}) = \sum_{n=1}^N \ell[n](\mu[n])$. The quantity $\ell[n](\mu[n])$ is the logarithm of $f(y[n], \mu[n])$ given by $\ell[n](\mu[n]) = \log\left(\frac{\pi}{2}\right) + \log(y[n]) - \log(\mu[n]^2) - \frac{\pi y[n]^2}{4\mu[n]^2}$, where $\mu[n] = g^{-1}\left(\sum_{i=1}^r x_i[n]\beta_i\right)$.

The score vector, obtained by differentiating the log-likelihood function with respect to each unknown parameters β_i , is given by $U(\boldsymbol{\beta}) = \left(\frac{\partial \ell(\boldsymbol{\beta})}{\partial \beta_1}, \frac{\partial \ell(\boldsymbol{\beta})}{\partial \beta_2}, \dots, \frac{\partial \ell(\boldsymbol{\beta})}{\partial \beta_r}\right)^\top$. Then, invoking the chain rule, we have

$$\frac{\partial \ell(\boldsymbol{\beta})}{\partial \beta_i} = \sum_{n=1}^N \frac{d\ell[n](\mu[n])}{d\mu[n]} \frac{d\mu[n]}{d\eta[n]} \frac{\partial \eta[n]}{\partial \beta_i},$$

where

$$\begin{aligned} \frac{d\ell[n](\mu[n])}{d\mu[n]} &= \frac{\pi y[n]^2}{2\mu[n]^3} - \frac{2}{\mu[n]}, \\ \frac{d\mu[n]}{d\eta[n]} &= \frac{1}{g'(\mu[n])}, \quad \frac{\partial \eta[n]}{\partial \beta_i} = x_i[n], \end{aligned} \quad (3)$$

and $g'(\cdot)$ is the first derivative of the adopted link function $g(\cdot)$. In particular, for the log link function, $g(\mu[n]) = \log(\mu[n])$, we have $\frac{d\mu[n]}{d\eta[n]} = \mu[n]$.

In matrix form, the score vector can be written as $U(\boldsymbol{\beta}) = \mathbf{X}^\top \cdot \mathbf{T} \cdot \mathbf{v}$, where \mathbf{X} is an $N \times r$ matrix whose n th row is $\mathbf{x}[n]^\top$, $\mathbf{T} = \text{diag}\left\{\frac{1}{g'(\mu[1])}, \frac{1}{g'(\mu[2])}, \dots, \frac{1}{g'(\mu[N])}\right\}$ and $\mathbf{v} = \left(\frac{\pi y[1]^2}{2\mu[1]^3} - \frac{2}{\mu[1]}, \frac{\pi y[2]^2}{2\mu[2]^3} - \frac{2}{\mu[2]}, \dots, \frac{\pi y[N]^2}{2\mu[N]^3} - \frac{2}{\mu[N]}\right)^\top$.

The maximum likelihood estimators (MLEs) for the Rayleigh regression parameters are obtained by solving the following nonlinear system:

$$U(\boldsymbol{\beta}) = \mathbf{0}, \quad (4)$$

where $\mathbf{0}$ is the r -dimensional vector of zeros. Solving (4) requires the use of nonlinear optimization algorithms. We adopted the quasi-Newton Broyden-Fletcher-Goldfarb-Shanno (BFGS) method [18] for the numerical computations. We suggest to use as initial point estimate for $\boldsymbol{\beta}$ the ordinary least squares estimate of $\boldsymbol{\beta}$, obtained from a linear regression of the transformed responses $g(y[1]), g(y[2]), \dots, g(y[N])$ on \mathbf{X} .

Based on the MLE of $\boldsymbol{\beta}$, it is possible to obtain a MLE for μ , considering the invariance principle of the MLE [17, Ch. 2], as $\hat{\mu} = g^{-1}(\mathbf{X}\hat{\boldsymbol{\beta}})$.

2.4 Goodness-of-fit Measures

In this section, diagnostic measures, such as the residual and the coefficient of determination, are presented to evaluate the correct adjustment of the proposed model. We considered the quantile residual as $r[n] = \Phi^{-1}(F(y[n]; \hat{\mu}[n]))$, where Φ^{-1} denotes the standard normal quantile function. The quantile residuals not only can detect poor fitting in regression models but its distribution is also approximately standard normal [3].

The generalized coefficient of determination [15], which is a global measure of the goodness-of-fit, is given by

$$R^2 = 1 - \exp\left(-\frac{2}{N} [\ell(\hat{\beta}) - \ell(\mathbf{0})]\right),$$

where $\ell(\mathbf{0})$ is the maximized log-likelihood of the null model (without regressors) and $\ell(\hat{\beta})$ is the maximized log-likelihood of the fitted model. Note that $0 \leq R^2 \leq 1$ and it indicates the proportion of the variability of the observed output signal that can be explained by the fitted model. Higher values of R^2 indicate more accurate predictions.

3 Detection Theory

It is possible to interpret a SAR image as a set of regions composed of possibly different types of probability laws [2]. The problem of correctly distinguishing between different regions in one image has been studied considering different statistical approaches. One approach to achieve this goal is the use of the hypothesis test, which allows for the computation of differences in the mean of the amplitude between two separate regions in a given image [2, 6]. In SAR image processing, this technique can also be considered for identification of land cover type, land cover change detection or classification, as shown in [5, 14].

3.1 Large Data Record Results

Under some mild regularity conditions [8, p. 167], the MLEs are consistent and asymptotically ($N \rightarrow \infty$) normally distributed. Thus, for large data record,

$$\hat{\beta} \sim \mathcal{N}_r\left(\beta, \mathbf{I}(\beta)^{-1}\right), \quad (5)$$

where $\mathbf{I}(\beta)$ is the Fisher information matrix. Their asymptotic distribution can be used to construct confidence intervals [17, Ch. 9] and hypothesis tests [17, Ch. 9].

To obtain the Fisher information matrix we need to calculate the expectation of the negative value of the second-order partial derivatives of the log-likelihood function [17, Ch. 8]. By applying the chain rule, the second-order derivatives of the $\ell(\beta)$ with respect to the β_i , $i = 1, 2, \dots, r$, are given by

$$\begin{aligned} \frac{\partial^2 \ell(\beta)}{\partial \beta_i \partial \beta_p} &= \sum_{n=1}^N \frac{d}{d\mu[n]} \left(\frac{d\ell[n](\mu[n])}{d\mu[n]} \frac{d\mu[n]}{d\eta[n]} \right) \frac{d\mu[n]}{d\eta[n]} \frac{\partial \eta[n]}{\partial \beta_p} \frac{\partial \eta[n]}{\partial \beta_i} \\ &= \sum_{n=1}^N \left(\frac{\partial^2 \ell[n](\mu[n])}{\partial \mu[n]^2} \frac{d\mu[n]}{d\eta[n]} + \frac{d\ell[n](\mu[n])}{d\mu[n]} \frac{\partial}{\partial \mu[n]} \right) \\ &\quad \times \frac{d\mu[n]}{d\eta[n]} \frac{d\mu[n]}{d\eta[n]} \frac{\partial \eta[n]}{\partial \beta_p} \frac{\partial \eta[n]}{\partial \beta_i}, \quad i, p = 1, 2, \dots, r. \end{aligned}$$

Note that taking expectation of (3), we have that $\mathbb{E}(d\ell[n](\mu[n])/d\mu[n]) = 0$. In addition, $\frac{\partial \eta[n]}{\partial \beta_p} = x_p[n]$, and $\frac{\partial \eta[n]}{\partial \beta_i} = x_i[n]$. Thus, $\mathbb{E}\left[\frac{\partial^2 \ell(\beta)}{\partial \beta_i \partial \beta_p}\right] = \sum_{n=1}^N \left[\mathbb{E}\left(\frac{d^2 \ell[n](\mu[n])}{d\mu[n]^2}\right) \left(\frac{d\mu[n]}{d\eta[n]}\right)^2 x_p[n] x_i[n] \right]$. Now, differentiating (3), we obtain $\frac{\partial^2 \ell[n](\mu[n])}{\partial \mu[n]^2} = \frac{2}{\mu[n]^2} - \frac{3\pi y[n]^2}{2\mu[n]^4}$. Taking the expected value, we have $\mathbb{E}\left[\frac{d^2 \ell[n](\mu[n])}{d\mu[n]^2}\right] = -\frac{4}{\mu[n]^2}$. Finally, we have $\mathbb{E}\left[\frac{\partial^2 \ell(\beta)}{\partial \beta_i \partial \beta_p}\right] = \sum_{n=1}^N \left[-\frac{4}{\mu[n]^2} \left(\frac{d\mu[n]}{d\eta[n]}\right)^2 x_p[n] x_i[n] \right]$. In matrix form, the Fisher information matrix is given by $\mathbf{I}(\beta) = \mathbf{X}^\top \cdot \mathbf{W} \cdot \mathbf{X}$, where $\mathbf{W} = \text{diag}\left\{\frac{4}{\mu[1]^2} \left(\frac{d\mu[1]}{d\eta[1]}\right)^2, \dots, \frac{4}{\mu[N]^2} \left(\frac{d\mu[N]}{d\eta[N]}\right)^2\right\}$.

3.2 Wald Test

To test hypotheses over the regression parameters, we partition the parameter vector $\beta = (\beta_I^\top, \beta_M^\top)^\top$, where β_I is the vector of parameters of interest with dimension ν and β_M is the nuisance parameter vector with dimension $r - \nu$. The hypothesis of interest is $\mathcal{H}_0 : \beta_I = \beta_{I0}$ versus $\mathcal{H}_1 : \beta_I \neq \beta_{I0}$. Here, β_{I0} is a fixed column vector of dimension ν . The Wald statistic can be written as [9, p. 190]:

$$T_W = (\hat{\beta}_{I1} - \beta_{I0})^\top \left(\left[\mathbf{I}^{-1}(\hat{\beta}_1) \right]_{\beta_I \beta_I} \right)^{-1} (\hat{\beta}_{I1} - \beta_{I0}),$$

where $\hat{\beta}_1 = (\hat{\beta}_{I1}^\top, \hat{\beta}_{M1}^\top)^\top$ is the MLE under \mathcal{H}_1 and $[\mathbf{I}^{-1}(\hat{\beta})]_{\beta_I \beta_I}$ is a partition of $\mathbf{I}(\hat{\beta})$ limited to the estimates of interest.

From (5) and based on the consistency of the MLE, the T_W statistic has an asymptotically chi-squared distribution with ν degrees of freedom, χ_ν^2 . The detection is performed by comparing the computed value of T_W with a threshold value γ obtained from the χ_ν^2 distribution and the desired probability of false alarm [9].

We assume that the mean of the Rayleigh distributed signal presents different values depending on the ground type. To illustrate, consider a region of forest in an image. The detection of this type of ground can be obtained by fitting the following Rayleigh regression model $g(\mu[n]) = \beta_1 + \beta_2 x_2[n] + \sum_{i=3}^r \beta_i x_i[n]$, where (i) β_1 is the intercept; (ii) $x_2[n]$ is a binary covariate equal to one if the region consists of forest and zero otherwise; and (iii) $x_i[n]$, $i = 3, 4, \dots, r$, are any other covariates that can influence the mean of y . The detection problem is to distinguish between the hypotheses:

$$\begin{cases} \mathcal{H}_0 : \mu[n] = g^{-1}(\beta_1 + \sum_{i=3}^r \beta_i x_i[n]), & (\beta_2 = 0), \\ \mathcal{H}_1 : \mu[n] = g^{-1}(\beta_1 + \beta_2 x_2[n] + \sum_{i=3}^r \beta_i x_i[n]). \end{cases} \quad (6)$$

To derive the detector, we can use the Wald test described above. We reject \mathcal{H}_0 when $T_W > \gamma$ [9]. In this situation, $\beta_2 \neq 0$ and the forest land use is detected. This technique can be considered to detect any type of ground in SAR images.

4 Numerical Results

This section presents Monte Carlo simulations and an empirical investigation in ground type detection in SAR images. The Monte Carlo simulations were used to evaluate the MLE of the Rayleigh regression parameters. An application with real SAR data was considered to demonstrate the proposed detector.

4.1 Analysis with Simulated Data

The numerical results are based on the Rayleigh regression model with the structure of the mean given by (2) considering the log link function. The parameters were adopted as follows: $\beta_1 = 2$, $\beta_2 = -1$, and $\beta_3 = 1$ for Scenario 1, and $\beta_1 = 0.5$ and $\beta_2 = 0.15$ for Scenario 2. The covariates were generated from the uniform distribution (0,1) and considered constants for all Monte Carlo replications. In each replication the inversion method was considered to generate $y[n]$ assuming the Rayleigh distribution with mean $\mu[n]$. The number of Monte Carlo replications was set equal to 10,000 and the signal lengths considered were $N \in \{25, 250, 1,000\}$.

We adopted the percentage relative bias (RB%) and the means square error (MSE) as figures of merit to numerically evaluate the proposed point estimators. Table 1 presents the simulation results. In general, we notice that the MLE of the Rayleigh regression model presented small values of percentage relative bias and mean square error. As expected, increasing N , the percentage relative bias and mean square error present lower values, which matches the consistence of the MLE.

Table 1: Results of the Monte Carlo simulation of the point estimation for Scenarios 1 and 2

	Scenario 1			Scenario 2	
Measures	β_1	β_2	β_3	β_1	β_2
$N = 25$					
Mean	1.9681	-1.0030	1.0040	0.4810	0.1472
RB(%)	1.5972	-0.3004	-0.4045	3.7913	1.8467
MSE	0.0909	0.1564	0.1533	0.0470	0.1421
$N = 250$					
Mean	1.9971	-1.0016	1.0009	0.4984	0.1489
RB(%)	0.1450	-0.1600	-0.0900	0.3200	0.7333
MSE	0.0073	0.0121	0.0126	0.0041	0.0125
$N = 1,000$					
Mean	1.9993	-1.0001	1.0002	0.4995	0.1502
RB(%)	0.0350	-0.0100	-0.0200	0.1000	-0.1333
MSE	0.0017	0.0030	0.0029	0.0010	0.0030

4.2 Analysis with Real Data

The SAR image considered in this application was taken by CARABAS II [12], a Swedish UWB VHF SAR system. The system uses HH polarization. All information related to the data can be found in [12, 22] and the images are available in [19]. The ground scene of the selected image is dominated by pine forest, fences, power lines, military vehicles, and roads; a lake is also present [12].

Figure 1 shows the three different regions representing forest, lake, and military vehicle imagery; referred to as Regions A1, A2, and A3, respectively. These regions were submitted to the proposed modeling and detector. The model is specified for the mean of the response signal using an intercept ($x_1[n] = 1$) and two dummy variables ($x_2[n]$ and $x_3[n]$) representing each tested region, as $g(\mu[n]) = \beta_1 + \beta_2 x_2[n] + \beta_3 x_3[n]$. The response signal is composed of the amplitude values of the pixels of the Regions A1, A2, and A3. Variable $x_2[n]$ is defined as one for Region A2 and zero for the rest. The variable $x_3[n]$ is defined as one for Region A3 and zero for the others. Region A1 is represented when $x_2[n] = 0$ and $x_3[n] = 0$.

For comparison purposes, we also fitted the standard Gaussian regression model, the GLM with Gamma distribution, and the Weibull regression model [28] to the Regions A1, A2, and A3. Detection with Gaussian distribution is widely discussed in literature and the Gamma and Weibull distribution are also used in SAR images, as in [23, 25]. The estimated parameters for the considered models are given in Table 2. In the Rayleigh regression model, the mean response presents a negative relationship with $x_2[n]$ and positive relationship with $x_3[n]$. Additionally, we notice that the lake and the target regions led to mean responses which are 12.05% lower and 194.00% higher than the mean response from the forest region, respectively.

The R^2 values of the fitted models show that the Rayleigh regression model can explain 70.96% of the variation in $y[n]$, while the Gamma GLM, Gaussian, and Weibull regression models can explain just 30.09%, 15.28%, and 0.3251%, respectively. Figure 2 presents the residuals of the Rayleigh regression model. As expected, the residuals present values close to zero for 98.81% of the observations and approximately standard normal distribution.

It is possible to define a detector for this specific regression model, based on (6). The detection problem in this image is based on computing the difference in the behavior among the tested regions. With the p -values of the Wald test presented in Table 2, we can verify that all variables in the Rayleigh regression model are significant for a probability of false alarm equal to 0.05. Hence, the null hypothesis in (6) can be rejected, indicating a correct detection of the land type. In contrast, the variable $x_2[n]$ is not significant for the Gamma GLM, Gaussian, and Weibull regression models, i.e., the Gaussian-, Gamma-, and Weibull-based detections can not distinguish the lake region from the other regions. Thus, the proposed Rayleigh regression model can be used for detecting differences in SAR image regions yielding more accurate results when compared to the competing regression models.

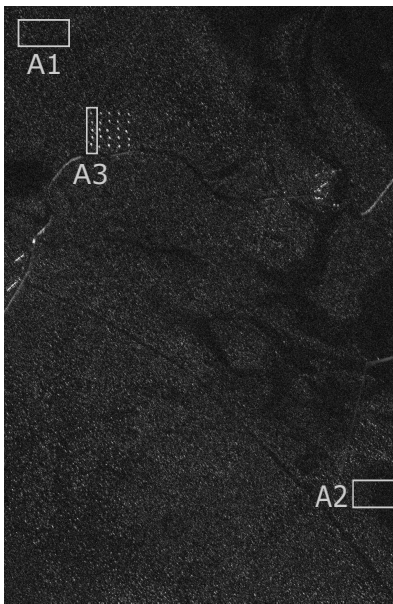


Figure 1: CARABAS II single-look image used in the regression models showing the regions tested. Regions A1, A2, and A3 represent a forest, a lake, and an area containing military vehicles, respectively.

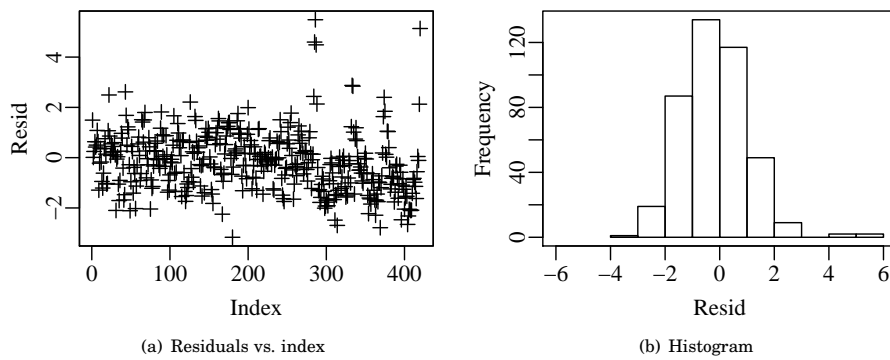


Figure 2: Residual charts for the Rayleigh regression model.

Table 2: Fitted regression models for Regions A1, A2, and A3

	Estimate	Standard Error	Detection (p -value)
Rayleigh regression model			
$\hat{\beta}_1$	-2.0623	0.0445	< 0.001
$\hat{\beta}_2$	-0.1280	0.0599	0.0325
$\hat{\beta}_3$	1.0784	0.0616	< 0.001
$R^2 = 0.7096$			
Gaussian regression model			
$\hat{\beta}_1$	0.12683	0.01646	< 0.001
$\hat{\beta}_2$	-0.01201	0.02213	0.588
$\hat{\beta}_3$	0.15948	0.02277	< 0.001
$R^2 = 0.1528$			
Gamma GLM			
$\hat{\beta}_1$	7.8844	0.5209	< 0.001
$\hat{\beta}_2$	0.8248	0.7341	0.262
$\hat{\beta}_3$	-4.3917	0.5657	< 0.001
$R^2 = 0.3009$			
Weibull regression model			
$\hat{\beta}_1$	-1.9939	0.0583	< 0.001
$\hat{\beta}_2$	-0.1157	0.0778	0.1373
$\hat{\beta}_3$	0.9583	0.0815	< 0.001
$R^2 = 0.3251$			

5 Conclusion

This letter introduced a new regression model for nonnegative signals. The proposed Rayleigh regression model assumes that the mean of the Rayleigh distributed signal follows a regression structure involving covariates, unknown parameters, and a link function. An inference approach for the model parameters is introduced and diagnostic tools are discussed. We also presented Fisher information matrix, asymptotic proprieties of the MLE, and a detector useful to detect differences in SAR image regions. In the Monte Carlo simulations, the MLE of the Rayleigh regression model showed small values of percentage relative bias and mean square error. An application of the Rayleigh regression model to distinguish between different regions in a SAR image was presented and discussed, showing more accurate detection results when compared with the measurements from Gaussian-, Gamma-, and Weibull-based regression models.

References

- [1] M. S. AMINZADEH, *Approximate 1-sided tolerance limits for future observations for the Rayleigh distribution, using regression*, IEEE Transactions on Reliability, 42 (1993), pp. 625–630.
- [2] R. J. CINTRA, A. C. FRERY, AND A. D. NASCIMENTO, *Parametric and nonparametric tests for speckled imagery*, Pattern Analysis and Applications, 16 (2013), pp. 141–161.
- [3] P. K. DUNN AND G. K. SMYTH, *Randomized quantile residuals*, Journal of Computational and Graphical Statistics, 5 (1996), pp. 236–244.
- [4] N. R. GOMES, M. I. PETTERSSON, V. T. VU, P. DAMMERT, AND H. HELLSTEN, *Likelihood ratio test for incoherent wavelength-resolution SAR change detection*, in 2017 IEEE Radar Conference (RadarConf), IEEE, 2017, pp. 1–4.
- [5] D. H. HOEKMAN AND M. J. QUIRIONES, *Land cover type and biomass classification using AirSAR data for evaluation of monitoring scenarios in the Colombian Amazon*, IEEE Transactions on Geoscience and Remote Sensing, 38 (2000), pp. 685–696.
- [6] J. INGLADA AND G. MERCIER, *A new statistical similarity measure for change detection in multitemporal SAR images and its extension to multiscale change analysis*, IEEE Transactions on Geoscience and Remote Sensing, 45 (2007), pp. 1432–1445.
- [7] J. A. JACKSON AND R. L. MOSES, *A model for generating synthetic VHF SAR forest clutter images*, IEEE Transactions on Aerospace and Electronic Systems, 45 (2009).

- [8] S. M. KAY, *Fundamentals of statistical signal processing: Estimation theory*, Prentice Hall PTR, 1993.
- [9] S. M. KAY, *Fundamentals of statistical signal processing: Detection theory*, vol. II, Prentice Hall, 1998.
- [10] E. E. KURUOGLU AND J. ZERUBIA, *Modeling SAR images with a generalization of the Rayleigh distribution*, IEEE Transactions on Image Processing, 13 (2004), pp. 527–533.
- [11] G. LAMPROPOULOS, A. DROSOPOULOS, N. REY, ET AL., *High resolution radar clutter statistics*, IEEE Transactions on Aerospace and Electronic Systems, 35 (1999), pp. 43–60.
- [12] M. LUNDBERG, L. M. H. ULANDER, W. E. PIERSON, AND A. GUSTAVSSON, *A challenge problem for detection of targets in foliage*, in Proc. SPIE, vol. 6237, 2006.
- [13] P. MCCULLAGH AND J. NELDER, *Generalized linear models*, Chapman and Hall, 2nd ed., 1989.
- [14] G. MERCIER, G. MOSER, AND S. B. SERPICO, *Conditional copulas for change detection in heterogeneous remote sensing images*, IEEE Transactions on Geoscience and Remote Sensing, 46 (2008), pp. 1428–1441.
- [15] N. J. NAGELKERKE ET AL., *A note on a general definition of the coefficient of determination*, Biometrika, 78 (1991), pp. 691–692.
- [16] C. OLIVER AND S. QUEGAN, *Understanding synthetic aperture radar images*, SciTech Publishing, 2004.
- [17] Y. PAWITAN, *In all likelihood: Statistical modelling and inference using likelihood*, Oxford, 2001. p. 528.
- [18] W. PRESS, S. TEUKOLSKY, W. VETTERLING, AND B. FLANNERY, *Numerical recipes in C: The art of scientific computing*, Cambridge University Press, 2 ed., 1992.
- [19] SDMS, *Sensor Data Management System public web site*, 2018. <https://www.sdms.afrl.af.mil/index.php>.
- [20] M. N. SUMAIYA AND R. S. S. KUMARI, *Unsupervised change detection of flood affected areas in SAR images using Rayleigh-based Bayesian thresholding*, IET Radar, Sonar & Navigation, 12 (2018), pp. 515–522.
- [21] G. TARICCO, *On the convergence of multipath fading channel gains to the Rayleigh distribution*, IEEE Wireless Communications Letters, 4 (2015), pp. 549–552.
- [22] L. M. ULANDER, M. LUNDBERG, W. PIERSON, AND A. GUSTAVSSON, *Change detection for low-frequency SAR ground surveillance*, IEEE Proceedings-Radar, Sonar and Navigation, 152 (2005), pp. 413–420.
- [23] V. T. VU, N. R. GOMES, M. I. PETERSSON, P. DAMMERT, AND H. HELLSTEN, *Bivariate gamma distribution for wavelength-resolution SAR change detection*, IEEE Transactions on Geoscience and Remote Sensing, (2018), pp. 1–9.
- [24] H. WANG AND K. OUCHI, *Accuracy of the k -distribution regression model for forest biomass estimation by high-resolution polarimetric SAR: Comparison of model estimation and field data*, IEEE Transactions on Geoscience and Remote Sensing, 46 (2008), pp. 1058–1064.
- [25] H. WANG, K. OUCHI, M. WATANABE, M. SHIMADA, T. TADONO, A. ROSENQVIST, S. A. ROMSHOO, M. MATSUOKA, T. MORIYAMA, AND S. URATSUKA, *In search of the statistical properties of high-resolution polarimetric SAR data for the measurements of forest biomass beyond the RCS saturation limits*, IEEE Geoscience and Remote Sensing Letters, 3 (2006), pp. 495–499.
- [26] A. WIESEL, Y. C. ELДАР, AND A. YEREDOR, *Linear regression with Gaussian model uncertainty: Algorithms and bounds*, IEEE Transactions on Signal Processing, 56 (2008), pp. 2194–2205.
- [27] M. ZANETTI, F. BOVOLO, AND L. BRUZZONE, *Rayleigh-rice mixture parameter estimation via EM algorithm for change detection in multispectral images*, IEEE Transactions on Image Processing, 24 (2015), pp. 5004–5016.
- [28] Z. ZHANG, *Parametric regression model for survival data: Weibull regression model as an example*, Annals of Translational Medicine, 4 (2016).